SELECTION OF REACTION MECHANISMS AND OF EXOTIC EVENTS IN HEAVY ION REACTIONS*

K. GROTOWSKI

M. Smoluchowski Institute of Physics, Jagellonian University
Reymonta 4, 30-059 Cracow, Poland

for the Grenoble-Lyon-Cracow Cooperation

M. Smoluchowski Institute of Physics, Jagellonian University
Reymonta 4, 30-059 Cracow, Poland
H. Niewodniczański Institute of Nuclear Physics
Radzikowskiego 152, 31-342 Cracow, Poland
Institut des Sciences Nucléaires de Grenoble
IN2P3-CNRS/ Université Joseph Fourier
53, Avenue des Martyrs, F-38046 Grenoble Cedex, France
Institut de Physique Nucléaire de Lyon
IN2P3-CNRS/ Université Claude Bernard
43, Boulevard du 11 Novembre 1918, F-69622 Villeurbanne Cedex, France

(Received December 10, 1996)

Problem of signatures of particular reaction mechanisms is discussed for the symmetric $^{40}Ca+^{40}Ca$ reaction at 35 MeV/nucleon. Special reaction filters are proposed. Some exotic events are presented.

PACS numbers: 25.70. Gh, 25.70. Lm, 25.70. Pq

1. Introduction

Since some time we know that nuclear matter exists in macroscopic quantities in the collapsing supernovas and in the resulting neutron stars. Thus hydrodynamic and thermodynamic properties of hot and cold nuclear matter are studied today with particular interest. Astrophysics needs information on nuclear matter compressibility, thermal expansion and more generally on its equation of state. Also interesting is the problem of phase transitions. We would like to know if critical phenomena in nuclear matter obey the same scaling relations as in other kinds of condensed matter.

* Presented at the XXXI Zakopane School of Physics, Zakopane, Poland, September 3–11, 1996.

Unfortunately, nuclear matter accessible for investigation is present only in microscopic quantities, inside atomic nuclei. In order to study nuclear thermodynamics one has therefore to collide together atomic nuclei and observe multifragmentation of produced in this way microscopic pieces of hot nuclear matter. Multiplicity, energy and angular distributions of different fragments, recorded event by event, correlated eventually with gamma rays, carry information on temperature, density of the excitation energy (pressure), entropy and other thermodynamic properties of hot nuclear matter. Such experiments demand large multidetector systems and complicated methods of data analysis, as well as time consuming computer simulations.

It has been recently realized that in the intermediate energy region, important for thermodynamics, mechanism of reactions producing hot nuclei is still not properly known. Consequently, selection of reaction scenarios leading to different multifragmentation sources is not an easy task. Multifragmentation is thought to be an important decay mode for composite systems created in central collisions, but also for the two highly excited fragments produced, at larger impact parameters, by the deep inelastic scattering (DIC) mechanism. In order to compare experimental data with predictions of various theoretical models it is therefore necessary to separate events corresponding to different reaction scenarios, occurring at different impact parameters. Special selection conditions (filters) imposed event by event on the data are employed for this purpose. Usually they make use of the so called violence of collision. For smaller impact parameters collisions become more violent, more particles are emitted, and they gain more momentum in the direction perpendicular to the initial beam of particles. The most obvious reaction filter could be the high multiplicity threshold, as in many cases exists a monotonic relation between mean multiplicity and impact parameter (angular momentum, L) [1]. Other observables used for construction of filters are also related to the violence of collision. Description of different reaction filters may be found in papers of Tsang *et al.* [2], Pèter *et al.* [3], and Brandon *et al.* [4].

In my talk I would like to discuss problems of separation of such collisions of identical ions, which produce hot composite nuclei. It is believed that they may provide information on hot nuclear matter, which expands after an initial compression. For discussion I shall use data obtained for the ^{40}Ca+^{40}Ca reaction at 35 MeV/nucleon. The data come from an experiment performed by the Grenoble, Lyon, Cracow cooperation [5, 6]. Measurements were made using the AMPHORA, 4π multidetector system [7]. For this experiment the AMPHORA system has been upgraded [8]. Instead of plastic scintillators, 30 gas ionization chambers were placed in front of the AMPHORA CsI(Tl) detectors, to lower energy thresholds for intermediate

mass fragments. To evaluate efficiency of different data sorting procedures I shall use predictions of an event generator.

2. Selection of well measured and well characterized events

Selection of a good sample of data is always of prime concern in any experiment. This trivial statement has a special meaning when multidetector systems, covering a solid angle close to 4π, are used. Each multifragmentation of an excited nucleus (an event) is here detected in some number of counters, which should identify particles and measure their energies or velocities. In the first step of data processing, after identification of particles and elimination of neutrons, gammas and randoms (by cleaning of the time spectra) one gets a sample of "well measured events".

In order to get complete information on a given reaction one should record complete events, it means such ones for which all fragments were detected and identified. Detection of complete events is not possible with the existing detector systems due to limitations of geometrical efficiency smaller from 100 percent, detector energy thresholds, and particle identification problems. *E.g.* in our case we detect charged particles only and identify their atomic number, Z. Consequently, in a real experimental environment one talks instead on "well characterized events" which carry a sufficient information. Definition of the sufficient information depends on the problem under investigation.

In our case we would like to recognize binary reaction products at larger impact parameters and composite system residues for more central collisions. The composite system residues are much more difficult to separate because of very small cross-sections. In the AMPHORA experiment the mean value of the total collected charge, Z_{tot}, is 22.3. We collect therefore in an event, on average, only about one half of the total charge $Z_0 = 40$, available in the entrance reaction channel. It is a consequence of the binary DIC scenario dominating in our reaction. Here some target-like fragments, TLF's, from peripheral collisions are not detected, because of energy thresholds or dead area of the detector system. We miss also some of projectile-like fragments, PLF's, escaping through the forward beam hole of AMPHORA. One can improve situation by imposing a condition on the total detected charge, *e.g.* $Z_{\mathrm{tot}} > 30$. For such "well characterized events" both binary reaction products will be seen in most cases, but the number of events is significantly reduced. In our experiment we get:

Recorded events	Well measured events	Well characterized events
$\approx 200 \times 10^6$ (1)	50×10^6 (25%)	3.5×10^6 (1.75%)

3. The event generator

The Monte Carlo event generator used by us permits both the DIC and the fusion (partial fusion) scenarios [9]. For each collision the interaction potential of colliding ions is computed and when there is no pocket in that potential it is treated as a DIC one, with a formation and subsequent deexcitation of two hot Ca-like fragments. The DI collision is described as a result of a random-walk transfer of nucleons and of the corresponding momentum between the projectile and the target [10]. The deexcitation of hot fragments is simulated using the GEMINI code [11]. For smaller impact parameters, when the system is trapped in the potential pocket a composite system is formed which afterwards decays. When larger angular momenta contribute to fusion the fission channel, which is kinematically similar to DIC, is favored. The border line between the DIC and the composite nucleus formation is located around $L = 100\,\hbar$, although the overlap region is quite broad. The above reaction picture may be supplemented by prompt emission of particles, PEP's (a midrapidity source).

To describe also particle–particle correlations the program numerically integrates equations of motion of all charged fragments in the mutual Coulomb field, allowing decays in flight [12].

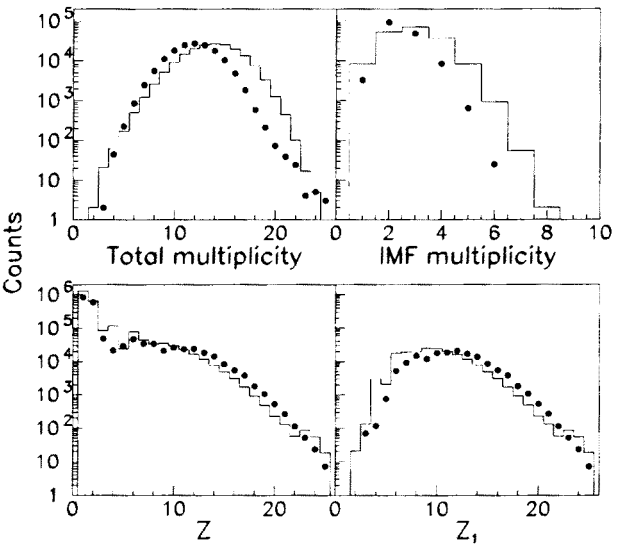

Fig. 1. Distributions of: charged particle multiplicity, IMF multiplicity, particle charge Z, charge Z_1 of the heaviest fragment. Well characterized events only. Black dots — experimental data, histograms — event generator.

Distributions of some global variables for well measured and well characterized events are presented in Fig. 1, and energy spectra in Figs 2(a) and 2(b). The solid lines show predictions of the event generator. In each case the influence of the AMPHORA detector system on model calculations was taken into account. As the predictions agree reasonably well with experimental data we shall use the event generator to test filters and reaction signatures.

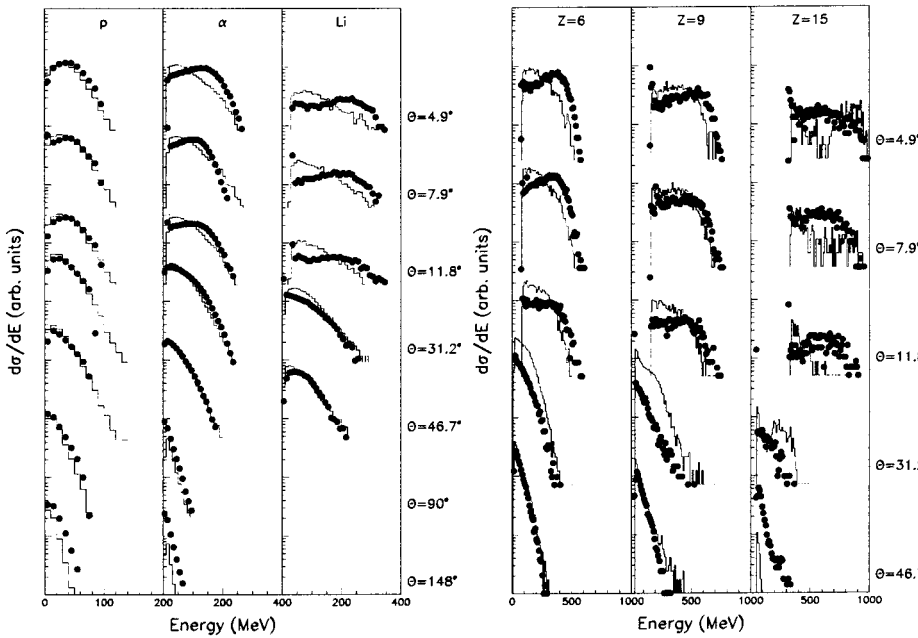

Fig. 2. Energy distributions of various ejectiles, at several LAB angles: (a) protons, α particles, *Li* ions; (b) $Z = 6, 9, 15$. Well characterized events. Black dots — experimental data, histograms — event generator.

4. Signatures of reaction scenarios

We shall look for special features of reaction mechanisms which could be observed in experimental data and used as signatures of different reaction scenarios.

In the DIC scenario one observes a projectile-like fragment, PLF, and a target-like fragment, TLF. They are the two heaviest fragments emitted in our ^{40}Ca+^{40}Ca reaction. As the collision is inelastic, kinetic energy of the entrance channel dissipates, the PLF and TLF get excited and evaporate particles. At the same time their linear momenta and relative velocity

decrease. Angular distribution of PLF's and TLF's is forward and backward peaked, respectively.

In the case of the composite system decay, the relative velocity of the two heaviest fragments depends rather on the system Coulomb barrier, only one source of emitted particles exists, and the CM angular distribution should be different.

Four signatures of the reaction scenario, making use of the above reaction features, will be discussed here.

4.1. Distribution of particle velocities in the v_{par}, v_{rel} plane

For each event, distribution of velocities of all $Z > 1$ particles is presented in a special plane, v_{par}, v_{rel}. Here v_{par} is a CM velocity projected on the $\vec{v_1} - \vec{v_2}$ axis and $v_{rel} = \mid \vec{v_1} - \vec{v_2} \mid$. Vectors $\vec{v_1}$ and $\vec{v_2}$ denote the velocity of the heaviest fragment detected in an event and of the second heaviest, respectively. For the symmetric $^{40}Ca + ^{40}Ca$ reaction the velocity vectors should be concentrated in two locations, around the PLF and TLF, for a DI collision but only in one location for the light particle (LP) and intermediate mass fragment (IMF) decay of a composite system (see contour plot in Fig. 3(a) for the DIC ($L > 150\,\hbar$; broken lines) and for the composite system decay ($L < 50\,\hbar$; solid lines), as predicted by the event generator).

4.2. Angular distribution of charged particles in the CM reference frame, oriented by $\vec{v_1}$ and $\vec{v_2}$

An angular distribution, $dN(\vartheta_{CM})/d\Omega$, of charged particles is plotted in the CM reference frame with the Z axis parallel to the vector $\vec{v_{rel}}$. Here ϑ_{CM} is the polar angle. For events from DIC's, the PLF and the TLF decay by emission of LP and IMF's, and in the CM velocity space one should observe two bundles of velocity vectors, contained inside two cones, oriented along $\vec{v_1}$ and $\vec{v_2}$, respectively. The velocity vectors should therefore exhibit an angular distribution with maxima in directions of $\vec{v_1}$ and $\vec{v_2}$. In this case, $dN(\vartheta)/d\Omega$ should have a concave shape, with maxima in the vicinity of 0 and 180 degrees (see Fig. 3(b); broken line).

For prompt decay from a compound nucleus, momentum conservation tends to produce a nearly back to back motion of the two heaviest fragments. This produces axial Coulomb focusing of light charged particles and thereby gives rise to a maximum in the $dN(\vartheta_{CM})/d\Omega$ distribution, at ϑ_{CM} close to 90 degrees [13]. This picture is modified by the AMPHORA filter producing a somewhat asymmetric distribution. In the case of sequential decay a broad, nearly flat distribution is observed (Fig. 3(b), solid line).

4.3. Distribution of the squared momentum of the heaviest fragment

The mean squared momentum, $\langle p_1^2 \rangle$, of the heaviest fragment (evaporation residue) for the sequential decay of a composite system can be deduced from a recursion relation derived by Cole [14]. In a mechanism similar to the Brownian motion random "kicks" from evaporated particles almost cancel each other. Consequently, the distribution of p_1^2 is narrow (Fig. 3(c), solid line). In the prompt multifragmentation case it is somewhat broader. Here the heaviest fragment is, on average, located closer to the surface than to the center of the initial configuration and a collective "kick" from the rest of

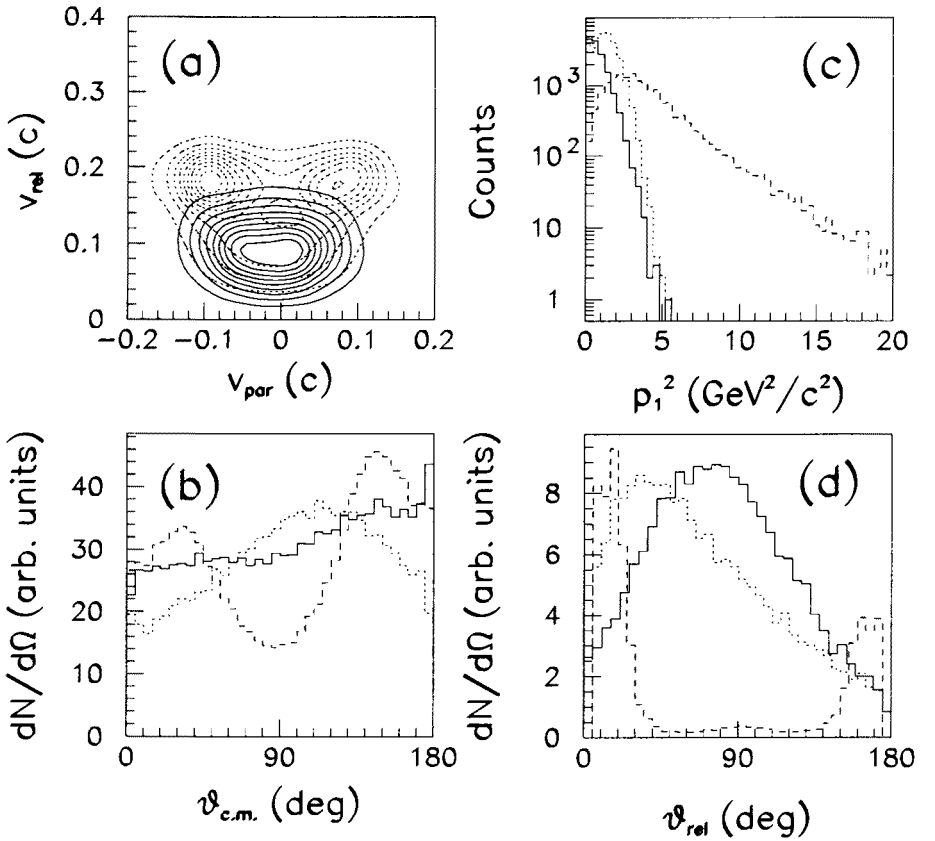

Fig. 3. Four signatures, predicted by the event generator and filtered by AMPHORA, for the DIC reaction ($L > 150\,\hbar$, broken lines), composite system sequential decay ($L < 50\,\hbar$, solid lines), and prompt multifragmentation ($L < 50\,\hbar$, dotted lines). (a) velocity distribution of $Z > 1$ particles in the $v_{\rm par}, v_{\rm rel}$ plane; (b) angular distribution in the CM reference frame oriented by the $\vec{v_{\rm rel}}$ vector; (c) p_1^2 distribution; (d) $dN(\vartheta_{\rm rel})/d\Omega$ distribution.

the decaying system creates a slightly larger $\langle p_1^2 \rangle$ (Fig. 3(c), dotted line). A broader distribution may be produced also by a radially directed collective movement [15] or the presence of angular momentum [16]. It is particularly broad for the DIC events where the projectile-like fragment and the target-like fragment have large relative momenta (Fig. 3(c), broken line). The width of the p_1^2 distribution depends here on the energy dissipation.

4.4. Distribution of events vs ϑ_{rel}

Fig. 3(d) shows the distribution of events $dN(\vartheta_{\mathrm{rel}})/d\Omega$, where ϑ_{rel} is the angle between $\vec{v_{\mathrm{rel}}}$ and the beam direction, predicted for DIC's by the event generator (broken line). Here, due to a forward-peaked angular distribution, characteristic of DIC's, for the majority of events ϑ_{rel} is either small or close to 180 degrees. The picture is different for LP or IMF decays of a composite system. Here, in principle, the distribution should be more flat but instead, after passing the AMPHORA filter, has a convex shape (solid line for the sequential decay and dotted line for the prompt multifragmentation).

Using signatures of the reaction mechanisms, described above, we can now try to find proper reaction filters to select or to eliminate events from different reaction scenarios.

5. Angular momentum (impact parameter) related filters

In heavy ion collisions, formation of a composite system takes place at low values of the relative angular momentum while at larger L values collisions become deep inelastic. One can try to employ L as a reaction filter. It is not easy to measure directly L but one can use instead some observable X which has a monotonic dependence on L. As X one frequently uses: the charge particle multiplicity, M, the total transverse momentum of charged particles in the direction perpendicular to the beam (or slightly differently defined directivity), the average particle velocity in the beam direction, or the midrapidity charge, which is the sum of all fragment charges for fragments with a rapidity intermediate between the projectile and target rapidities (see *e.g.* [3]).

It has been demonstrated, using the reaction signatures of Sec. 4, that for such symmetric heavy ion reaction, as our Ca + Ca , the high multiplicity threshold alone, and other L related filters, are not sufficient to distinguish composite system decays from DIC's (see [5, 6]). The reason is, a very broad L *vs* X event distribution, and below $L = 100\,\hbar$ a very weak (or even a non-monotonic) $\langle L \rangle$ *vs* X dependence. An additional difficulty in using *e.g.* the M-threshold as a filter are randoms which are due to two events occuring in one beam burst [6].

6. Reaction filters making use of special reaction features

As the L related filters can not be applied we have to make use of special event features which differentiate the composite system formation from the DIC scenario. They are *e.g.* event shapes in momentum space, relative velocity of the two heaviest fragments, the linear momentum of the heaviest fragment, and so on. We propose here two filters which will be nick-named: the "sphere" filter and the "triangle" filter.

6.1. The "sphere" filter

We introduce a coordinate system X, Y, Z with: $x = p_1/p_p; v_{\rm rel}/v_{pt}$; $z = \varepsilon$. Here p_p, v_{pt} and ε is the projectile momentum, the entrance channel projectile-target relative velocity and the event elongation ε in the momentum space (see next section), respectively. We define a global variable ρ [6] as:

$$\rho = \sqrt{x^2 + y^2 + z^2}\,. \tag{1}$$

Each event is represented now by a point in the X, Y, Z space. Its dimensionless coordinates x, y, z have values from zero to one. It is clear, that for nearly central collisions events should be located close to the origin of the coordinate system (small ρ values). For DIC's and quasi elastic collisions one expects events up to $\rho = 3^{1/3}$.

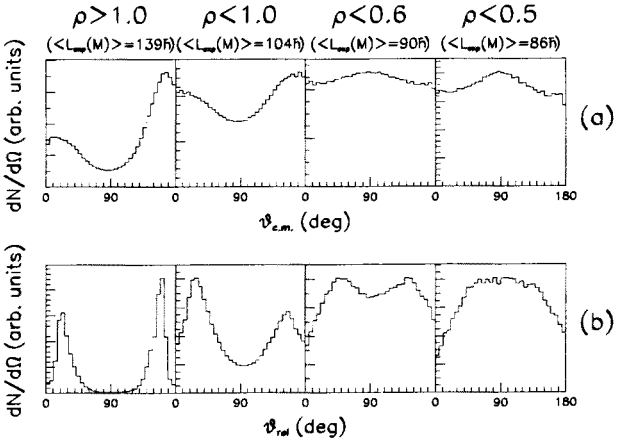

Fig. 4. Two signatures (as Fig. 3(b), 3(d)) obtained from experimental data for well characterized events and the "sphere" filter with different ρ values. The corresponding $< L_{\rm exp}(M) >$ values are given in parenthesis.

In Fig. 4 two of our signatures are presented for measured, well characterized events, which have passed the "sphere" filter. For $\rho > 1$ we see

a concave $dN(\vartheta_{\rm CM})/d\Omega$ distribution, and a $dN(\vartheta_{\rm rel})/d\Omega$ distribution with two maxima at small and large angles, both characteristic of DIC. For decreasing ρ values the picture transforms into the one expected for the composite system decay (compare Figs 3(a) and (b)). In particular, for $\rho < 0.5$, the $dN(\vartheta_{\rm CM})/d\Omega$ distribution has now a convex shape and the minimum in $dN(\vartheta_{\rm rel})/d\Omega$ gradually disappears, finally forming a broad maximum located at intermediate angles. We do not present here two remaining signatures as they are directly correlated with the "sphere" filter.

6.2. The "triangle" filter

This filter uses global variables: sphericity, S, and coplanarity, C, related to the shape of each multifragmentation event in the linear momentum space (see [5, 6]).

In order to describe event shapes in the space of the linear momentum one uses the linear momentum tensor [17]:

$$F_{ij} = \frac{\sum_1^M \frac{p_i^{(n)} p_j^{(n)}}{|p^{(n)}|}}{\sum_1^M \mid p^{(n)} \mid}, \tag{2}$$

where $p_i^{(n)}$ is the i-th Cartesian momentum component of the n-th fragment, and $\mid p^{(n)} \mid$ is the length of the momentum vector. For $t_1 < t_2 < t_3$, (the ordered eigenvalues of the tensor F) one defines the reduced quantities:

$$q_i = \frac{t_i^2}{\sum_1^3 t_j^2}. \tag{3}$$

Now, for each event, one can introduce sphericity $S = \frac{3}{2}(1 - q_3)$, coplanarity $C = \frac{1}{2}3^{1/2}(q_2 - q_1)$, and event elongation $\varepsilon = 1 - S^{1/2}$. In the S, C plane each event is represented by a point located inside a triangle with coordinates: (0,0), (1,0) and $(3/4, 3^{1/2}/4)$. For $(S, C) = (1, 0)$ the momentum surface defined by the linear momentum tensor has a spherical shape, for $(3/4, 3^{1/2}/4)$ it has a disc shape, and for (0,0) it is like a rod-like object. In an infinite multiplicity approximation, events from central collisions are represented by the (1,0) point, and from DIC's by the (0,0) point. For limited multiplicities of our reaction they are smeared over quite a large region, but not the same for both reaction scenarios. The larger the value of M, the better the distinction between them. We know however that random events begin to dominate for too large M. In our case, $M_{\rm th} = 16$ seems to be a safe value [6].

Fig. 5 presents the S, C map of well characterized, measured events. We propose a filter which together with the $M_{th} = 16$ condition accepts only

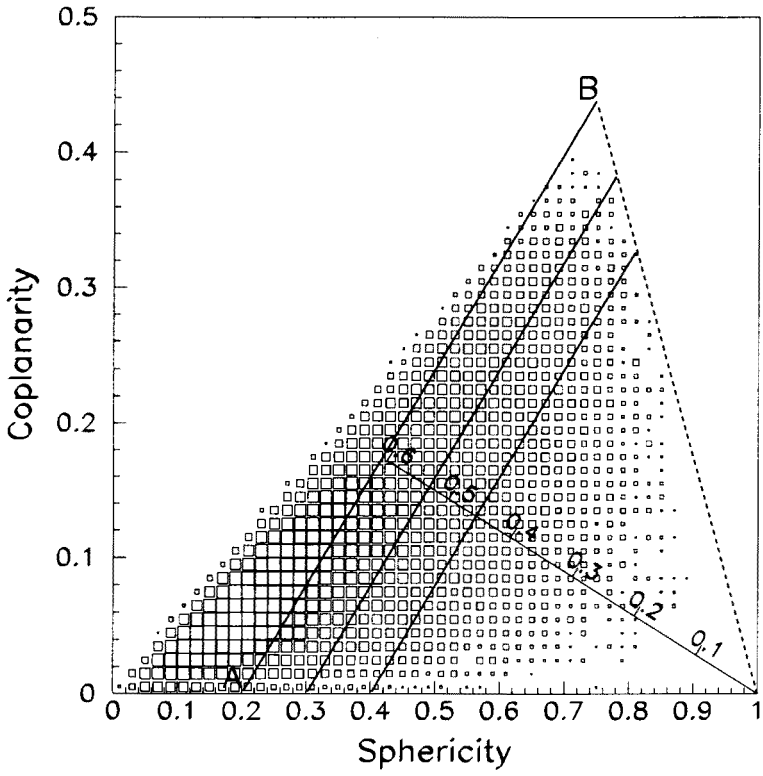

Fig. 5. Map of well characterized events ($M \geq 16$) in the S, C plane (see text).

those events which are located inside a triangle $A, B, (1,0)$. Location of the AB line is given by a "distance" d, from the (1,0) point (see Fig. 5). Simulations suggest that decays of the composite system predominate in the right part of the picture.

In Fig. 6 application of the filter to experimental data is demonstrated. For events located outside the $d = 0.61$ triangle we see a picture characteristic of the DIC reaction, but already with a significant contribution from the formation of a composite system (a hill at $v_{\mathrm{par}} \cong 0$). Here the DIC events are seen as two ridges at $v_{\mathrm{rel}} \cong 0.15$ (Fig. 6(a)). For decreasing d values one observes a transition toward: one event hill in the $v_{\mathrm{par}}, v_{\mathrm{rel}}$ plane (Fig. 6(a)); a convex $dN(\vartheta_{CM})/d\Omega$ distribution (Fig. 6(b)); and a fairly narrow $p_{\perp}^2$ distribution (Fig. 6(c)). For the $dN(\vartheta_{\mathrm{rel}})/d\Omega$ distribution (Fig. 6(d)) two maxima observed at small and large ϑ_{rel}, respectively (larger d values) evolve towards one broad structure at $d < 0.46$.

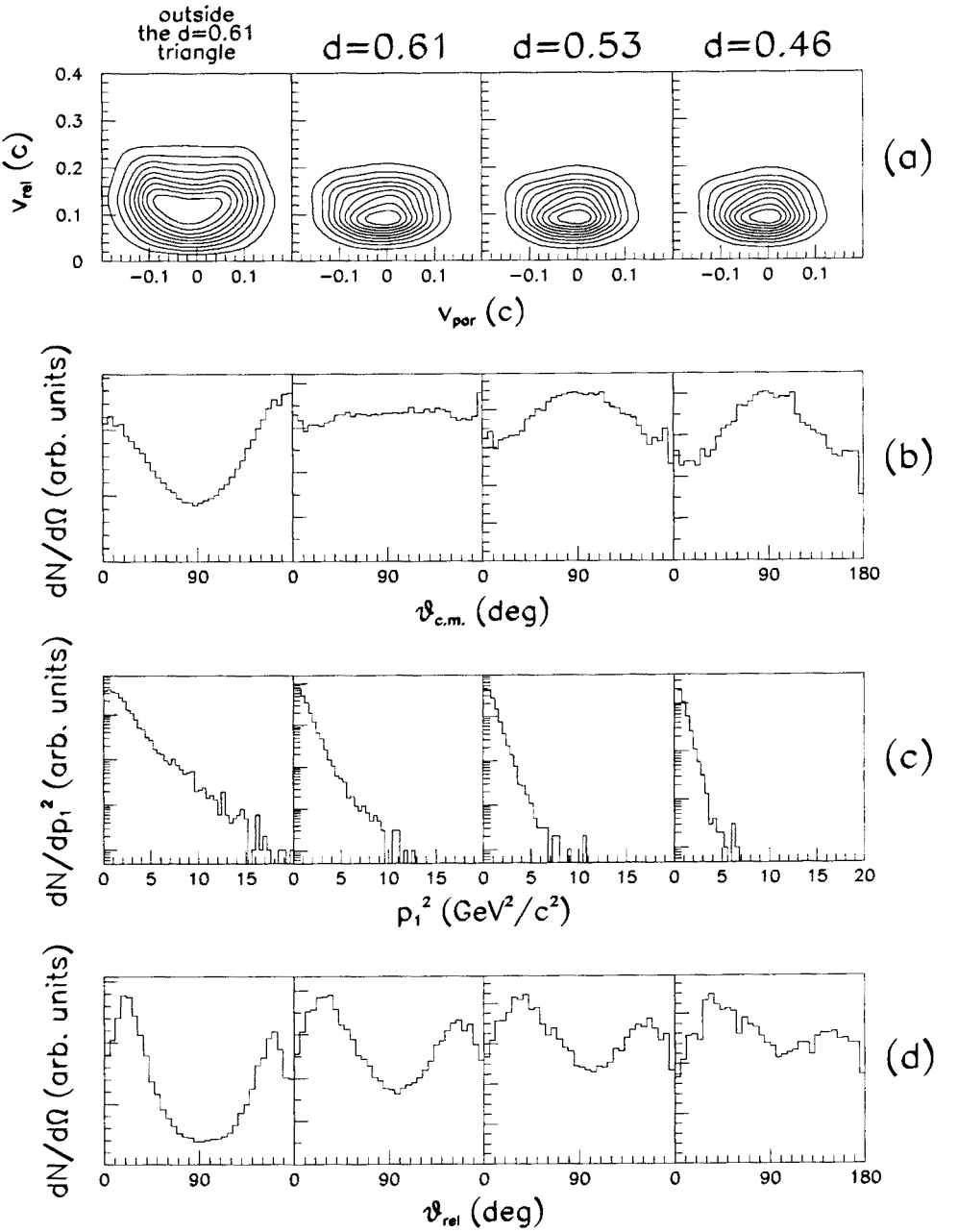

Fig. 6. Four signatures (as Fig. 3) obtained from experimental data for well characterized events and the "triangle" filter with $M \geq 16$ and different d values.

7. Great problem ! ... number of events

Using two special filters, "sphere" and "triangle", we were able to select events which, as suggested by the reaction signatures, come from decays of hot composite systems. Due to different definitions, "sphere" and "triangle" select slightly different groups of events. Contrary to its nickname, the "triangle" filter allows more "spherical" events to pass, favouring decays with emission of LP's and IMF's. The "sphere" filter gives more chance also to the "fusion-fission" type of decays. Both filters let some of the DIC events to pass (about 30 percent for $\rho < 0.5$, or $d < 0.46$; predicted by the event generator). That admixture comes from such DIC events at large energy dissipation which have shapes similar to these from composite system decays.

At this discrimination level the number of transmitted events is very small. It may be seen from the following table:

Recorded events	Well measured events	Well characterized events	After filters (events)
$\approx 200 \times 10^6$ (1)	50×10^6 (25%)	3.5×10^6 (1.75%)	$\rho < 0.52 \rightarrow 2.3 \times 10^5$ ($\approx$0.1%) $d < 0.46 \rightarrow 1.7 \times 10^4$ ($\approx$0.01%)

These final numbers are so small, partly due to imperfection of our filters, but first of all they are a consequence of very small cross-sections for formation of composite systems. (see *e.g.* [3]). The "sphere" filter lets more events to pass than the "triangle" one. It is so because the fusion-fission events as no-spherical in shape are forbidden by the the "triangle" filter.

Summarizing the first part of my talk I would like to stress the following points:

(i) Selection of events from decays of composite systems produced in collisions of symmetric ions, like Ca + Ca, is difficult, due to very small cross-sections and a rather complicated reaction picture.

(ii) One needs here special reaction signatures and reaction filters.

(iii) Although one can say that the number of events on the level of 1.75×10^4 or 2.3×10^5 is satisfactory for comparison with models and further analysis, but in order to obtain them one has to begin from about 2×10^8 events recorded on magnetic tapes.

8. Selection of exotic events — can one observe toroidal nuclei?

Almost 50 years ago, in the unpublished "Nucleonics Notebook" Wheeler suggested existence of toroidal nuclei [18]. About 30 years ago Siemens and Bethe discussed existence of bubble nuclei [19]. Ten years ago Wong pointed out that probability of existence of such nuclei should depend on temperature [20].

It is supposed today that such exotic shapes could be eventually created in nucleus-nucleus collisions, however they will promptly decay into nearly equal IMF's. Relation of this effect to the Rayleigh– Taylor-like surface instability was discussed by Moretto, Wozniak and others for disc, toroidal and bubble systems [21]. Formation and decay of such systems was studied in a number of BUU, percolation model, and other calculations at MSU, Texas $A\&M$, Caen, Nantes and other places (see [22] and references therein).

Having a reasonable number of events recorded in our ^{40}Ca+^{40}Ca experiment we got tempted to look for events from decays of such exotic nuclei into some number of nearly equal IMF's.

We define the heaviest IM fragment, the second heaviest, and so on as: $Z_1, Z_2, \ldots Z_i$, respectively. Now a set of "equal" fragments in an event is given by the condition:

$$Z_1 - Z_i \leq 1, \quad z_i > 2\,. \tag{4}$$

For analysis only half of the full sample of 3.5×10^6 well characterized events was used. It contains 1343 events with 4 "equal" IMF's. If such exotic structures exist one should expect them rather in nearly central collisions, although it is not clear how central they should be. We began with the "sphere" filter and $\rho < 0.52$, getting 170 events. Fig. 7, where distributions of Z_1 up to Z_4 are presented, explains why this number is so small. It is clear that selection of "flat" objects, as discs or toroids, is easier than of the bubble ones. Identification of "flat" objects, consisting of some number of "equal" fragments may be performed in a simple way. A plain, for which the distance from the vector tips of the 4 "equal" IMF's is the smallest one, is found for each case. The 4 IMF system is "flat" when that distance, on the average, is smaller from 16 percent of their average length projected on the plane. Such an arbitrary choice is a compromise between a perfect flatness of objects and angular granularity of AMPHORA ($\delta\vartheta \cong 4°, \delta\phi \cong 15°$ wall; $\delta\vartheta \cong 15°, \delta\phi \cong 24°$ ball).

For 4 "equal" fragments ($\rho < 0.52$) there are 78 "flat" objects. The center of mass (cm) points of these "flat" objects are fairly well centered around the reaction center of mass, CM.

As typical examples, the momentum vectors of four "flat" objects projected on their respective planes, are presented in Fig. 8. Events displayed

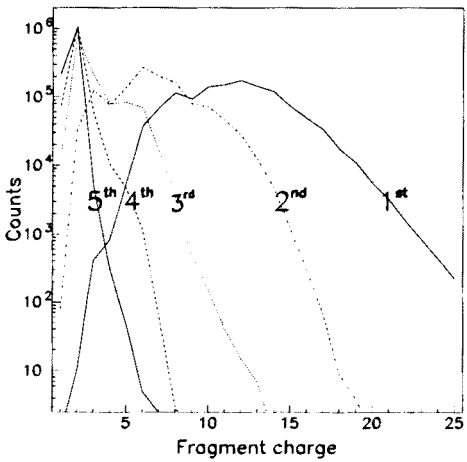

Fig. 7. Experimental Z distributions for the heaviest IM fragment, the second heaviest, and so on, up to $Z_i = 5$.

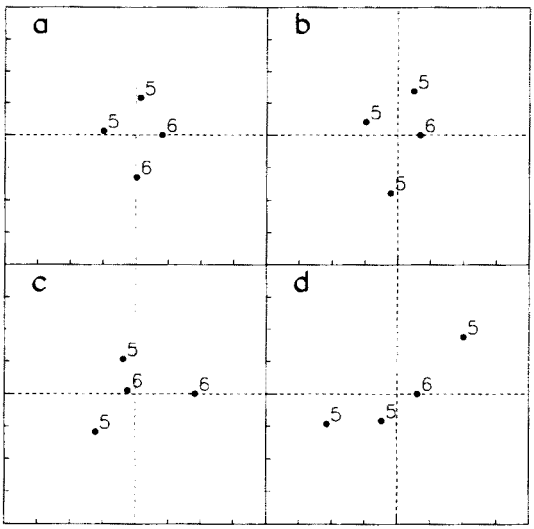

Fig. 8. The momentum vectors of "flat" objects (4"equal" fragments) projected on their respective planes (see text).

in Figs 8a and 8b could be attributed to decays of toroidal systems, events from Fig. 8c to decays of disc structures, and events from Fig. 8d to a "background" of badly measured events. We have got 17, 20 and 41 events in

the first, second and third category, respectively. The average Z contained in four "equal" fragments of "flat" objects is 21, what is about half of the available charge. The corresponding average energy per nucleon is 2.5 MeV (cm).

The total multiplicity of all these events is about 13. In CM, the four "equal" fragments have, on average, 2–3 times longer linear momentum vectors than the rest of particles in an event (with the exception of some PEP's). Consequently, these events look really exotic, like the Saturn with its ring (Fig. 9). We see a nearly spherical structure of momentum vectors from lighter particles, and a "flat" structure of longer momentum vectors from "equal" intermediate mass fragments.

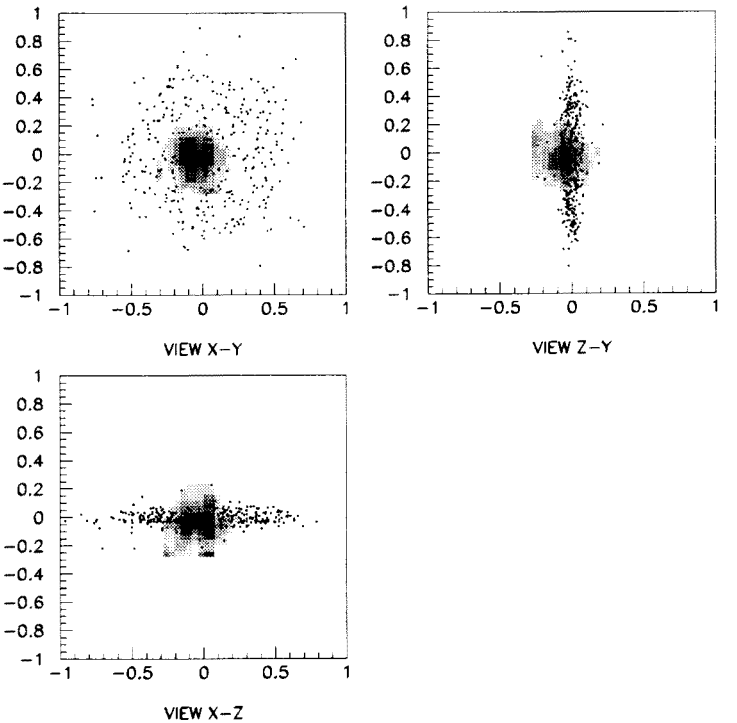

Fig. 9. Projection of the spatial distribution of the momentum vectors of exotic events on the XY, YZ, and XZ plane, respectively.

Fig. 10 presents locations of these exotic events in the sphericity, coplanarity plane. In Fig. 10(a) the S, C coordinates were calculated using momenta of all particles in an event. The events are distributed between the $(0,0) - (3/4, 3^{1/2}/4)$ line, and the $A, B(d = 0.46)$ line. Only very few of them are present inside the $A, B, (1,0)$ triangle, as the exotic events are

not "spherical". In Fig. 10(b) linear momenta of the four "equal" fragments only were taken. Here the events concentrate very close to the $(0,0)-(3/4, 3^{1/2}/4)$ line, because they represent flat objects.

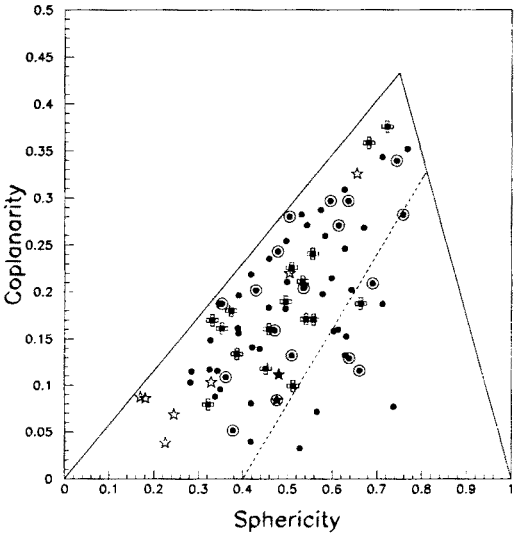

(a)

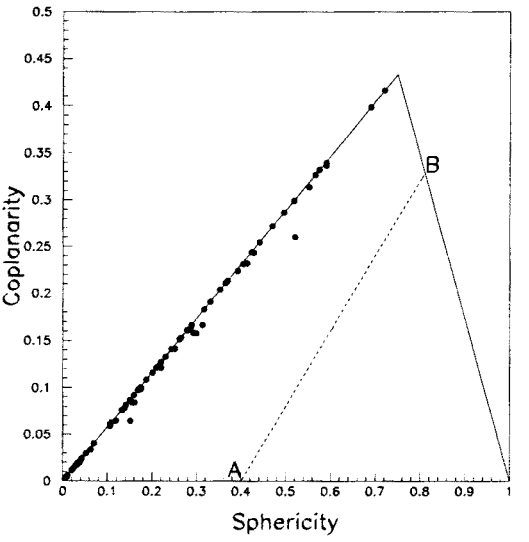

(b)

Fig. 10. Distribution of exotic events in the S, C plane: (a) using momenta of all particles in an event; (b) using momenta of "equal" fragments only.

At this moment I would like to make a statement:

We do not claim observing decays of transitional shapes, either disc-like nor toroidal-like. We only say that we see events which look like coming from such exotic objects. One has to keep in mind that they are very scarce and may also come from some "strange" DIC, fusion-fission or fusion-evaporation events. With all restrictions imposed in selection of these exotic events, the upper limit of the corresponding cross-section is about 5 mb.

This statement is signed by all members of the cooperation: D. Benchekrovn, E. Bisquer, J. Brzychczyk, A. Chabane, M. Charvet, B. Cheynis, A.J. Cole, A. Demeyer, P. Desesquelles, W. Gawlikowicz, E. Gerlic, A. Giorni, K. Grotowski, D. Guinet, P. Hachaj, D. Heuer, P. Lautesse, L. Lebreton, A. Lléres, S. Micek, P. Pawłowski, R. Płaneta, Z. Sosin, M. Stern, L. Vagneron, J.B. Viano, and A. Wieloch.

The presented work was supported by the Polish-French (I N_2 P_3) agreement and the Polish State Committee for Scientific Research (KBN Grant No. PB 719/P3/93/04).

REFERENCES

[1] C. Cavata, M. Demoulins, J. Gosset, M.C. Lemaire, D.L. Hote, J. Poitou, O. Valette, *Phys. Rev.* **C42**, 1760 (1990); Y.D. Kim, R.T. de Souza, D.R. Bowman, N. Carlin, C.K. Gelbke, W.G. Gong, W.G. Lynch, L. Phair, M.B. Tsang, F. Zhu, *Phys. Rev.* **C45**, 338 (1992).

[2] M.B. Tsang, G.F. Bertsch, W.G. Lynch, M. Tohyama, *Phys. Rev.* **C40**, 1685 (1989).

[3] J. Péter, S.C. Jeong, J.C. Angélique, G. Auger, G. Bizard, R. Brou, A. Buta, C. Cabot, Y. Cassagnou, E. Crema, D. Cussol, D. Durand, Y. El Masri, P. Eudes, Z.Y. He, A. Kerambrun, C. Lebrun, R. Legrain, J.P. Patry, A. Péghaire, R. Régimbart, E. Rosato, F. Saint-Laurent, J.C. Steckmeyer, B. Tamain, E. Vient, *Nucl. Phys.* **A593**, 95 (1995).

[4] M.E. Brandan, A.J. Cole, P. Désesquelles, A. Giorni, D. Heuer, A. Lléres, A. Menchaca-Rocha, K. Michaelian, *Nucl. Instrum. Methods* **A334**, 461 (1993).

[5] P. Pawłowski, D. Benchekrovn, E. Bisquer, J. Brzychczyk, A. Chabane, M. Charvet, B. Cheynis, A.J. Cole, A. Demeyer, P. Desesquelles, W. Gawlikowicz, E. Gerlic, A. Giorni, K. Grotowski, D. Guinet, P. Hachaj, D. Heuer, P. Lautesse, L. Lebreton, A. Lléres, S. Micek, R. Płaneta, Z. Sosin, M. Stern, L. Vagneron, J.B. Viano, A. Wieloch, *Phys. Rev.* **C54**, R10 (1996).

[6] P. Pawłowski, D. Benchekrovn, E. Bisquer, J. Brzychczyk, A. Chabane, M. Charvet, B. Cheynis, A.J. Cole, A. Demeyer, P. Desesquelles, W. Gawlikowicz, E. Gerlic, A. Giorni, K. Grotowski, D. Guinet, P. Hachaj, D. Heuer, P. Lautesse, L. Lebreton, A. Lléres, S. Micek, R. Płaneta, Z. Sosin, M. Stern, L. Vagneron, J.B. Viano, A. Wieloch, sent for publication in *Z. Phys.*

[7] D. Drain, A. Giorni, D. Hilscher, C. Ristori, J. Alaria, G. Barbier, R. Bertholet, R. Billerey, B. Chambon, B. Cheynis, J. Crançon, A. Dauchy, P. Désesquelles, A. Fontenille, L. Guyon, D. Heuer, A. Lléres, M. Maurel, E. Monnand, C. Morand, H. Nifenecker, C. Pastor, J. Pouxe, H. Rossner, J. Saint-Martin, F. Schussler, P. Stassi, M. Tournier, J.B. Viano, *Nucl. Instrum. Methods* **A281**, 528 (1989).

[8] T. Barczyk, J. Brzychczyk, P. Burzyński, W. Gawlikowicz, K. Grotowski, S. Micek, P. Pawłowski, R. Płaneta, A.J. Cole, A. Chabane, P. Désesquelle, A. Giorni, D. Heuer, A. Lléres, J.B. Viano, D. Benchekroun, B. Cheynis, A. Demeyer, E. Gerlic, D. Guinet, P. Lautesse, L. Lebreton, M. Stern, L. Vagneron, *Nucl. Instrum. Methods* **A364**, 311 (1995).

[9] Z. Sosin, A. Wieloch, prepared for publication.

[10] Z. Sosin, K. Grotowski, A. Wieloch, H.W. Wilschut, *Acta Phys. Pol.* **B25**, 1601 (1994); Z. Sosin, J. Brzychczyk, K. Grotowski, J.D. Hinnefeld, E.E. Koldenhof, H.K.W. Leegte, J. Lukasik, S. Micek, R.H. Siemssen, A. Wieloch, H.W. Wilschut, *Nucl. Phys.* **A574**, 474 (1994).

[11] R.J. Charity, M.A. McMahan, G.J. Wozniak, R.J. McDonald, L.G. Moretto, D.G. Sarantites, L.G. Sobotka, G. Guarino, A. Pantaleo, L. Fioe, A. Gobbi, K.D. Hildebrand, *Nucl. Phys.* **A483**, 371 (1988).

[12] W. Gawlikowicz, ISN Rep. 95-129.

[13] W. Gawlikowicz, K. Grotowski, *Acta Phys. Pol.* **B22**, 885 (1991); *Nucl. Phys.* **A551**, 73 (1993).

[14] A.J. Cole, M.E. Brandan, P. Désesquelles, A. Giorni, D. Heuer, A. Lléres, A. Menchaca-Rocha, J.B. Viano, B. Chambon, B. Cheynis, D. Drain, C. Pastor, *Phys. Rev.* **C47**, 1251 (1993).

[15] D. Heuer, A. Chabane, M.E. Brandan, M. Charvet, A.J. Cole, P. Désesquelles, A. Giorni, A. Lléres, A. Menchaca-Rocha, J.B. Viano, D. Benchekroun, B. Cheynis, A. Demeyer, E. Gerlic, D. Guinet, M. Stern, L. Vagneron, *Phys. Rev.* **C50**, 1943 (1994).

[16] A.S. Botvina, D.H.E. Gross, *Nucl. Phys.* **A592**, 257 (1995).

[17] J. Cugnon *et al.*, *Phys. Lett.* **B109**, 167 (1982); M. Gyulassy, K.A. Frankel, H. Stöker, *Phys. Lett.* **B110**, 185 (1982); G. Fai, J. Randrup, *Nucl. Phys.* **A404**, 551 (1983).

[18] J.A. Wheeler, Nucleonics Notebook, 1950, unpublished.

[19] P. Siemens, H. Bethe, *Phys. Rev. Lett.* **18**,704 (1967).

[20] C.Y. Wong, *Phys. Rev. Lett.* **55**, 1973 (1985).

[21] L.G. Moretto, Kin Tso, N. Colonna, G.J. Wozniak, *Phys. Rev. Lett.* **69**, 1884 (1992); L.G. Moretto, Kin Tso, G.J. Wozniak, LBL Rep. 34724, 1993.

[22] W. Bauer, G.F. Bertsch, H. Schulz, *Phys. Rev. Lett.* **69**, 1888 (1992); D.H.E. Gross *et al. Ann. Phys.* **1**, 467 (1992); B. Borderie *et al.*, Université Paris Rep. I.P.N.-91406, 1992; T. Glasmacher, C.K. Gelbke, S. Pratt, Rep. MSUCL-893, 1993; L. Phair, W. Bauer, C.K. Gelbke, Rep. MSUCL-890, 1993; H.M. Xu, J.B. Natowitz, C.A. Gagliardi, R.E. Tribble, C.Y. Wong, W.G. Lynch; D. Durand, J.F. Lecolley, M. Aboufirassi, R. Bougault, J. Colin, A. Genoux-Lubain, C. LeBrun, O. Lopez, M. Louvel, C. Meslin, G. Rudolf, L. Stuttgé, S. Tomasevic, ISMRA Rep., 1995.